J. Fluid Mech. (1992), *vol.* 242, *pp.* 193–209
Printed in Great Britain

The capillary instability of annular layers and liquid threads

By LORI A. NEWHOUSE AND C. POZRIKIDIS
Department of Applied Mechanics and Engineering Sciences, 0411, University of California, San Diego, La Jolla, CA 92093, USA

(Received 24 June 1991 and in revised form 3 February 1992)

The capillary instability and break-up of an annular liquid layer coating the inner surface of a cylindrical tube while surrounding another core fluid is studied. In the limiting case where the thickness of the layer is almost equal to the radius of the tube, we obtain a thread of core fluid suspended in a virtually unbounded ambient liquid. The evolution of a layer or thread with a cylindrical or unduloidal interface subject to an axisymmetric perturbation is computed using a boundary integral method. It is shown that for large and moderate layer thicknesses the instability causes the core to transform into an alternating array of primary and secondary spherical drops along the centreline of the tube. The relative volume of the drops depends primarily on the ratio of the core radius to the tube radius, a/R, and the type of initial perturbation. The evolution of thin layers with $a/R > 0.82$ leads to formation of an array of lobes or collars. These results are used to assess the accuracy of previous approximate analyses based on lubrication flow and minimization of interfacial area.

1. Introduction

When a fluid displaces a liquid in a porous medium or through a channel, it leaves behind a fluid layer that coats the grains of the porous medium or the walls of the channel. After the flow has stopped, the layer evolves under the action of hydrodynamic instabilities due to gravitational and capillary forces. Roughly speaking, the evolution due to capillary forces may lead to formation of two types of structure: pendant or sessile lobes, also termed collars, and lenticular bridges. The former are attached to the surface of the host solid medium, and the latter extend across and occlude the passages of the host medium. The type of emerging structure depends primarily on the relative magnitudes of the thickness of the layer and the characteristic length and radius of curvature of the channels of the host medium.

To develop an understanding of the behaviour of a coated liquid layer, it is useful to consider a simple model consisting of an annular laying lining the inner surface of a straight cylindrical tube, while the core of the tube is occupied by another fluid. The annular layer not only provides us with a viable working model, but also is directly relevant to the behaviour of the gel that coats the micro-airways of the lungs (George *et al.* 1990; Johnson *et al.* 1991). The collapse of this gel and consequent occlusion of bronchioles signals the onset of respiratory problems and allows the multiplication of infectious organisms. When the thickness of the annular layer is almost equal to the radius of the tube, the core reduces to a thin thread, and the effect of the tube on the motion of the interface becomes insignificant. The instability and break-up of fluid threads are relevant to a broad class of chemical engineering

processes involving the dispersion and mixing of immiscible fluids (Khakhar & Ottino 1987).

One way to assess the behaviour of an annular layer is to study its stability subject to controlled perturbations. In the unperturbed state, the layer is assumed to be in hydrostatic equilibrium where the mean curvature of the interface between the layer and the core is constant. Uniform mean curvature implies constant jump in the pressure across the interface, absence of pressure variations within the layer, and lack of a driving mechanism for the deformation of the interface. Restricting our attention to smooth axisymmetric and periodic interfaces we find a family of hydrostatic shapes, termed unduloids, produced by rolling an ellipse along the centreline of a cylindrical tube and identifying the trace of one focus of the ellipse with the interface between the layer and the core (Everett & Haynes 1972). When the ellipse degenerates to a sphere, the trace is a straight line corresponding to a cylindrical core. An ellipse with large eccentricity resembles a straight segment, the trace is a sequence of circles, and the core is composed of an array of touching spheres.

Goren (1962) investigated the linear instability of a cylindrical annular layer coating the inner or outer surface of a cylinder subject to axisymmetric disturbances, for the case where the viscosity of the core or ambient fluid vanishes. His computations revealed that the layer is always unstable to sufficiently long waves, and there is a finite wavelength with maximum growth rate. In the limit where the radius of the core becomes small, his results reduce to those of Tomotika (1936) for a thread of viscous fluid suspended in another unbounded liquid. Everett & Haynes (1972) studied the stability of stationary annular collars with unduloidal interfaces and found that there is a maximum volume above which a collar might become unstable and transform into a lenticular bridge. Their work was motivated by the physics of capillary condensation in porous media. More recently, Georgiou *et al.* (1991) studied the linear instability of an annular film of an electrolyte coating the inner surface of a cylindrical tube including both capillary and electrostatic forces.

The nonlinear evolution and rupture of annular films was studied in the laboratory by Goldsmith & Mason (1963), Goren (1964), Everett & Haynes (1972), and more recently by Gauglitz & Radke (1988). The experiments of Goren involved coating the cylindrical wire and recording the subsequent evolution of the interface. All other experiments were conducted by introducing a long bubble into a liquid residing in a cylindrical tube, and observing the subsequent evolution of the interface. Gauglitz & Radke, in particular, showed that a thin annular film breaks up into a combination of collars and bridges, and presented data for the number of developed lenses as a function of the thickness of the annular layer.

The nonlinear evolution of a stationary annular layer was studied theoretically on several occasions using approximate methods. Goren (1964) computed transient shapes of an annular layer coating the exterior of a cylindrical tube. In his analysis, he neglected the effect of the fluid flow, stipulated that the surface area of the interface is minimum for given layer volume and amplitude of the free surface, and regarded the amplitude of the free surface as a known function of time. His computations showed that the instability leads to formation of periodic toroidal collars connected by thin cylindrical bridges, in good agreement with his experimental observations. Goren noted that his quasi-hydrostatic model is also applicable for annular layers coating the inner surface of the tube.

Hammond (1983) used the lubrication approximation to devise a model for describing the evolution of a thin annular film, and found that the breakup of the film

may lead to formation of several primary and secondary collars of varying dimensions within one wavelength of the perturbation. One interesting finding is that, at large times, the axial dimension of the primary collars tends to the value $2\pi R$, where R is the radius of the tube, independently of the wavelength of the initial perturbation. Gauglitz & Radke (1988) improved the accuracy of Hammond's equations, and computed a critical film thickness above which the instability of the layer leads to formation of bridges instead of collars. Their results will be discussed further in §3. Johnson *et al.* (1991) developed an integral method for thin films based on the boundary-layer approximation including the effects of inertia, and studied the characteristic time for bridge formation. The results were discussed in the context of pulmonary pathology.

From a more general perspective, the capillary instability of a stationary annular layer may be considered as a special case of the instability of the interface between two co-flowing fluids arranged in a core–annulus configuration. Recently, there has been renewed interest in this more general problem, motivated primarily by applications in lubricated pipelining. Linear and weakly nonlinear stability analyses were carried out by Russo & Steen (1989) and Hu & Joseph (1989), and the nonlinear evolution of thin layers was computed by Papageorgiou, Malderelli & Rumschitzki (1990).

In this work we study the capillary instability of a stationary annular layer coating the inner surface of a circular tube when the layer is subjected to axisymmetric disturbances and the flow occurs under conditions of creeping motion. Our objective is to present an integrated parametric investigation which will extend and bridge the gaps between the asymptotic cases considered by previous authors and will allow us to evaluate the accuracy of approximate analyses. We consider the behaviour of annular layers with cylindrical and unduloidal interfaces, study the evolution of layers or arbitrary thickness, and describe the motion for large interfacial deformations up to, and after the point where the core breaks up to form arrays of collars or lenses. For layers of small thickness, we compare our results with predictions of approximate analyses based on the assumption of lubrication flow. To treat the limiting case of a layer whose thickness is nearly equal to the radius of the tube, we consider the evolution of an unbounded thread in an infinite ambient fluid. By comparing the evolution of a thread to that of a core, we are able to study the precise effect of the wall on the qualitative and quantitative features of evolution.

Our analysis is based on numerical solutions of the equations of creeping flow and is carried out using a boundary integral method (Pozrikidis 1992*a*). One novel feature of our formulation is the use of an axisymmetric period Green's function that vanishes over the cylinder. Using this Green's function, we are able to express the velocity field as an integral over the trace of the interface in a meridional plane.

In the case of the suspended thread we shall consider situations where the viscosity of the suspending fluid is different to that of the thread. In the case of the annular layer, however, we shall confine our attention to situations in which the viscosity of the core is equal to that of the annular fluid, as this permits a critical simplification in our numerical procedure. At first sight, it might appear that the assumption of equal viscosities is quite specialized. Previous experience, as well as present computations for the thread, however, indicate that this case is typical of those where the viscosity of the core is smaller than or comparable to that of the annular fluid (Pozrikidis 1990). This is certainly true in the case of thin annular layers, as shown rigorously in the asymptotic analysis of Hammond (1983).

2. Problem formulation and solution

We consider the evolution of an axisymmetric annular layer of viscosity μ wetting the inner surface of a cylindrical tube while surrounding another core fluid with viscosity $\lambda\mu$, when it is subjected to axisymmetric disturbances of wavelength L. Gravitational forces are assumed to be negligible compared to capillary forces and thus, they are overlooked. When the radius of the tube, R, is large compared to the radius of the core, a, we obtain a thread suspended in an infinite ambient fluid.

In the absence of an imposed axial flow the annular layer might assumed a hydrostatic configuration in which the mean curvature of the interface is constant. Such configurations are provided by a cylindrical core and the more general case of a core whose interface is an unduloid, constructed by rolling an ellipse along the centreline of the tube. We seek to assess the stability of these hydrostatic configurations by computing the linear and nonlinear evolutions of the layer subject to axisymmetric disturbances.

When the thickness of the annular layer is comparable to the radius of the core, an effective Reynolds number of the flow due to the instability may be defined as $J = \rho\gamma R/\mu^2$, where γ is the interfacial tension (Goren 1962). Johnson *et al.* (1991) discuss the effective Reynolds number for thin annular layers. Assuming that the effective Reynolds number is small, we neglect inertial effects in the flow and introduce a boundary integral representation applicable for Stokes flow. Thus, we express the velocity as a distribution of the fundamental flow due to a ring of point forces over one period of the trace of the interface in an azimuthal plane, C, as

$$u_\alpha(x_0) = \int_C \boldsymbol{M}_{\alpha\beta}(x_0, x)\, q_\beta(x)\, \mathrm{d}l(x) \tag{2.1}$$

where $\boldsymbol{M}$ is the axisymmetric Green function that vanishes over the tube and is periodic in the axial direction with period L, and Greek subscripts take the values x and σ to indicate, respectively, the axial and radial directions. The function $\boldsymbol{q}$ represents the density of the ring distribution. The derivation and computation of $\boldsymbol{M}$ are discussed by Pozrikidis (1992*a*, *b*) and Newhouse (1991). Requiring continuity of velocity across the interface and the usual boundary condition for the jump in surface force across the interface, we obtain the following Fredholm integral equation of the second kind for $\boldsymbol{q}$

$$q_\alpha(x_0) = -\frac{1}{4\pi\mu_1(1+\lambda)}\gamma[2k_{\mathrm{m}}\, n_\alpha](x_0) + \frac{\beta}{4\pi} n_\beta(x_0) \int_C^{PV} Q_{\beta\delta\alpha}(x_0, x)\, q_\delta(x)\, \mathrm{d}S(x) \tag{2.2}$$

where the point x_0 lies on C, $\beta = (\lambda-1)/(\lambda+1)$, k_{m} is the mean curvature of the interface, $\boldsymbol{Q}$ is a singular kernel, and PV indicates the principal value of the integral. Details of the boundary integral representation are given by Pozrikidis (1990, 1992 *a*). Our numerical procedure involves solving (2.2) for $\boldsymbol{q}$ using Picard iterations, and then computing the velocity field using the defining equation (2.1).

Owing to the complicated nature of the kernel $\boldsymbol{Q}$ in the case of an annular layer, we shall consider only the case $\lambda = 1$ or $\beta = 0$ for which the coefficient in front of the integral in (2.2) vanishes, and $\boldsymbol{q}$ is equal to the first term on the right-hand side. In the case of a suspended thread we shall consider evolutions for other values of λ. The numerical procedure involves tracing the interface with a set of marker points, computing the velocity, and advancing the position of the marker points. Details are given by Newhouse (1991). All calculations were executed on the CRAY-Y/MP

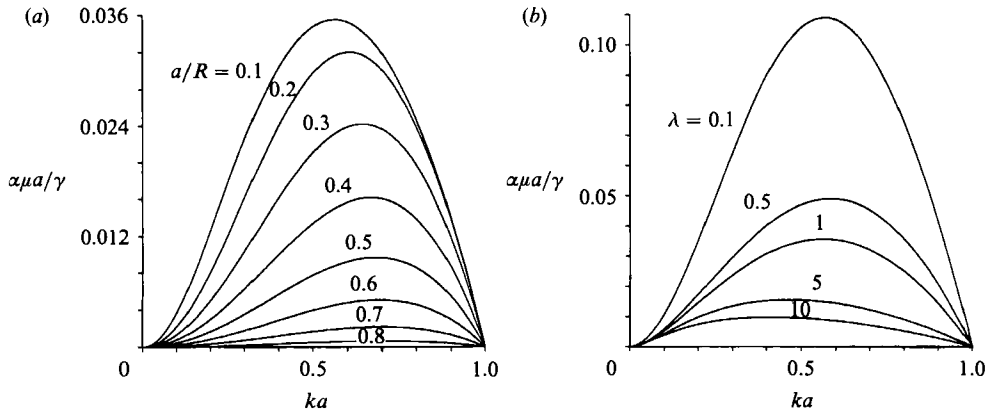

FIGURE 1. The reduced linear growth rate of a cylindrical annular layer of core radius a wetting the inner surface of a tube of radius R, as a function of the reduced wave number ka; (*a*) the effect of core radius for viscosity ratio $\lambda = 1$; (*b*) the effect of λ for a thread, $a/R = 0$.

computer of the San Diego Supercomputer Center. A complete computation required as much as 8 h of CPU time.

3. Results and discussion

We begin our studies by considering the initial growth of small axisymmetric disturbances using standard linear stability theory. Thus, we introduce axisymmetric perturbations which are proportional to $\exp(\alpha t + ikx)$, where α is the growth rate and k is the wavenumber, and after neglecting inertial effects, we derive a relation of the form $\alpha\mu a/\gamma = F(\lambda, ka, a/R)$, where F is an involved function of its arguments. The derivation and exact form of F are presented by Georgiou *et al.* (1991) and Newhouse (1991).

In figure 1(*a*) we plot the reduced growth rate $\alpha\mu a/\gamma$ as a function of ka for $\lambda = 1$ and several values of the radii ratio a/R. We observe that short wavelength disturbances with $ka > 1$ are stable, long wavelength disturbances with $ka < 1$ are unstable, and the critical wavenumber for incipient stability $ka = 1$ is independent of the ratio a/R. As the radius of the core is increased, $a/R \to 1$, that is, the thickness of the annular layer is decreased, the growth rate is markedly reduced. These results confirm our physical intuition that the presence of the wall has a strong stabilizing effect on the behaviour of thin annular films. It is interesting to note that the wavenumber with maximum growth rate is rather insensitive to the value of a/R. To examine the effect of the viscosity ratio λ, in figure 1(*b*) we plot the reduced growth rate for a suspended thread, $a/R = 0$, as a function of ka for several values of λ. Clearly, as λ is increased and the core becomes more viscous, the growth rate is reduced and the wavenumber with maximum growth rate shifts to smaller values. Georgiou *et al.* (1991) show that inertial effects act to reduce the growth rate of the disturbance.

We consider next the evolution of small perturbations beyond the linear growth regime using the boundary integral method. In our investigation, we seek to describe the growth of the most unstable perturbation for given values of a/R and λ. Unless stated otherwise, we consider perturbations whose reduced wavenumber ka corresponds to the maximum growth rate according to linear theory. At the outset, we non-dimensionalize our variables using as characteristic length the inverse

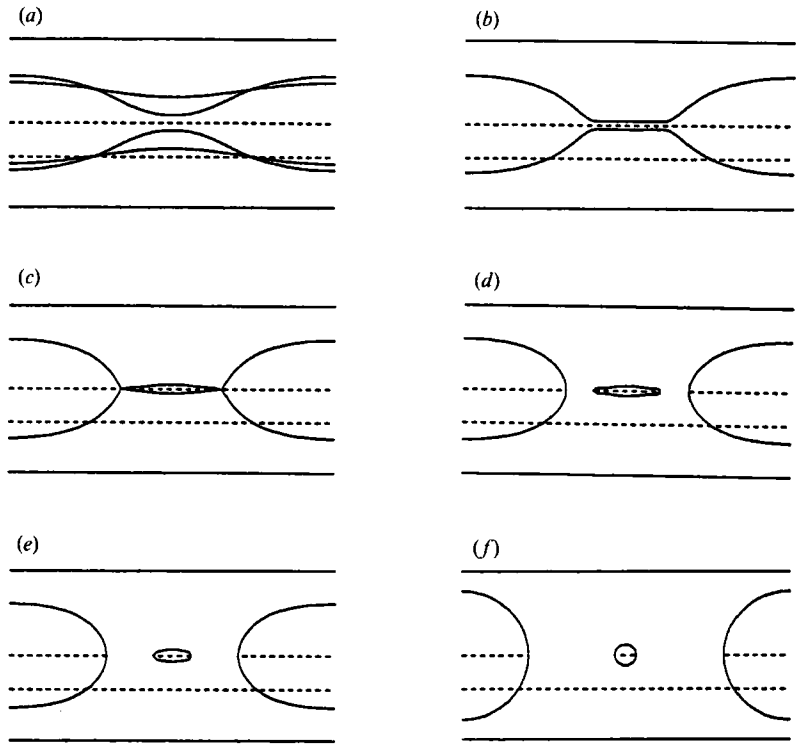

FIGURE 2. Characteristic stages in the evolution of an annular layer with $a/R = 0.40$ and $\lambda = 1$ for the most unstable perturbation at (*a*) $t = 265, 308$, (*b*) $t = 314$, (*c*) $t = 317$, (*d*) $t = 319$, (*e*) $t = 320$, (*f*) $t = \infty$.

wavenumber $1/k$ and characteristic time $\mu a/\gamma$. In dimensionless variables, the motion is a function of the core radius ka, the radii ratio a/R, and the viscosity ratio λ. For annular layers we shall present results only for $\lambda = 1$, whereas for unbounded threads we shall consider the motion for several other values of λ.

3.1. *The case* $\lambda = 1$

In figure 2 we present characteristic stages in the evolution of the most unstable perturbation $ka = 0.6679$ for an annular layer with $a/R = 0.4$. Each frame shows one period of the interface. The upper and lower solid horizontal lines represent the surface of the tube, the upper dashed line represents the centreline, and the lower dashed line represents the position of the unperturbed interface. In the first stage of evolution, the core develops an hour-glass shape with a thinning neck and a thickening end (figure 2*a*). In the second stage, the core transforms into a series of primary drops which are linked by nearly cylindrical threads (figure 2*b*). The third stage begins with a bulging of the threads and subsequent formation of slender drops with pointed ends (figure 2*c*). To continue this calculation it was necessary to disconnect the primary drops from the slender secondary drops at that point in time where the interface crossed the centreline, owing to numerical error. In reality, the process and time of breakup will be determined by a local dynamics which is dominated by intermolecular forces, but these are not included in our formulation.

In figures 2(*d*, *e*) we illustrate the evolution after breakup. After the slender secondary drops have been disconnected, they shrink and obtain a compact shape under the action of surface tension. The contraction of the slender drops occurs on

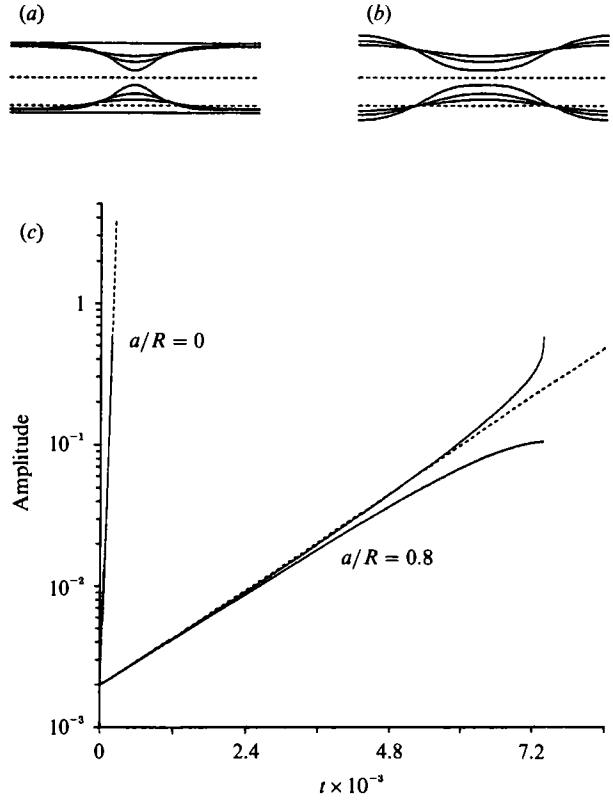

FIGURE 3. (*a*) Characteristic stages in the evolution of an annular layer with $a/R = 0.80$ and $\lambda = 1$ subjected to the most unstable perturbation at $t = 6473, 7188, 7381$; (*b*) corresponding stages in the evolution of an unbounded thread at $t = 134, 153, 167$; (*c*) the evolution of the amplitude of the trough (upper solid line) and crest (lower solid line) of the interfacial wave. ---, predictions of linear theory.

a timescale much shorter than that of the development of the link-drop structure. During the contraction process, the boundary of the slender drops develops a wavy pattern which indicates the onset of a secondary capillary instability. Our calculations suggest, however, that this instability does not have a permanent effect on the long-time behaviour of these drops. At large times, the core is expected to obtain a composite shape that consists of an alternating sequence of primary and secondary spherical drops, as illustrated in figure 2(*f*).

The evolution of layers with $a/R < 0.4$ is quite similar to that illustrated in figure 2(*a–f*), involving the development of the drop-link structure and the reduction of the core to an alternating series of primary and secondary spherical drops. The wall has a minor influence on the qualitative features of the evolution as well as the timescale of the instability.

In figure 3(*a*), we present characteristic stages in the evolution of a thin layer $a/R = 0.8$ for $ka = 0.7014$. To illustrate the effect of the wall, in figure 3(*b*) we show corresponding stages of an unbounded thread, $a/R = 0$. In the presence of the tube the trough of the interface is much sharper, the primary drop is more elongated, and the link is shorter. These observations suggest that the wall acts not only to slow down the motion, by almost two orders of magnitude, but also to modify the geometry of the emerging structures. At large times, the link depicted in figure 3(*a*) is expected to collapse at the centreline forming an axisymmetric lenticular bridge.

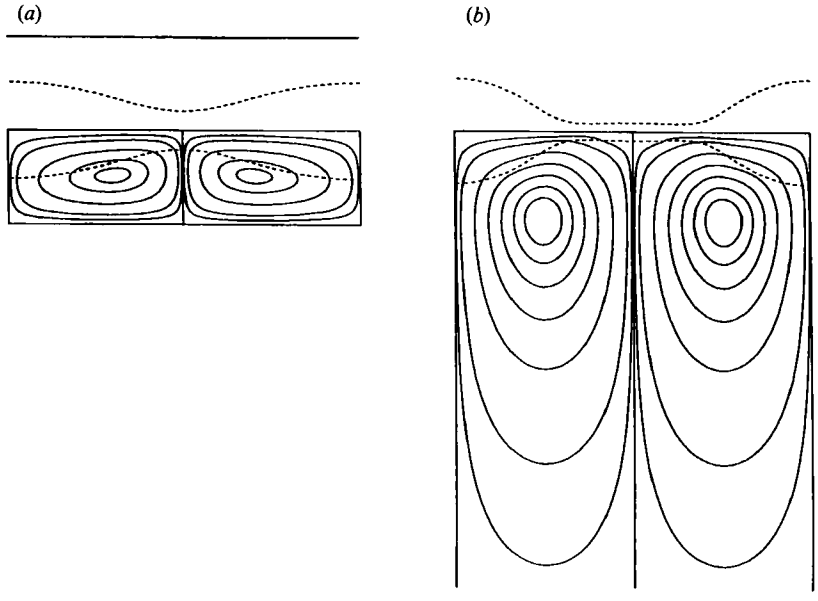

FIGURE 4. Instantaneous streamline patterns for (a) an annular layer with $a/R = 0.40$, $ka = 0.668$ at $t = 292$, (b) a thread with $ka = 0.562$ at $t = 108$.

Next, we discuss the motion in a more quantitative sense. In figure 3(c) we plot the amplitudes of the crest and trough of the interface on a semi-logarithmic scale, corresponding, respectively, to the maximum and minimum core radii, for the evolutions illustrated in figure 3(a, b). The dashed line represents the predictions of linear stability theory, the upper solid line represents the trough close to the centreline, and the lower solid lines represents the crest close to the wall. There is an excellent agreement between the numerical results and the predictions of linear stability theory at the initial stages of motion, and a fair agreement at the advanced stages of motion where the interface no longer has a sinusoidal shape. It is worth noting that our computations predict a faster growth of the trough and a slower growth of the crest in the advanced stages of motion. The prominent differences in the magnitude of the slopes for $a/R = 0.8$, and 0 is evidence of the strong influence of the wall.

Figure 3(c) indicates that linear instability analysis might provide us with a fairly accurate estimate of the bridge formation, or breakup time. We find that this is true especially for layers of moderate and large thickness. A convenient measure of the breakup time is the time at which the thickness of the core midway between two primary drops is minimum; after this time, the connecting link starts bulging, transforming into a slender drop. We thus compute the ratio of the actual breakup time to that predicted by linear theory as a function of a/R for the most unstable mode. This ratio is approximately 1.09 for the unbounded thread, $a/R = 0$, decreases to approximately 1 at $a/R = 0.2$, and continues decreasing to 0.82 at $a/R = 0.8$.

To obtain further insights into the kinematics of the transient flow, in figure 4 we present instantaneous streamline patterns for an annular layer with $a/R = 0.40$ and an unbounded thread, $a/R = 0$. In both cases we observe a symmetric set of two counter-rotating eddies driving fluid away from the connecting links into the developing primary drops.

In all of the cases considered so far, the instability has led to breakup of the core into an array of primary drops which are separated by bridges of annular fluid. At

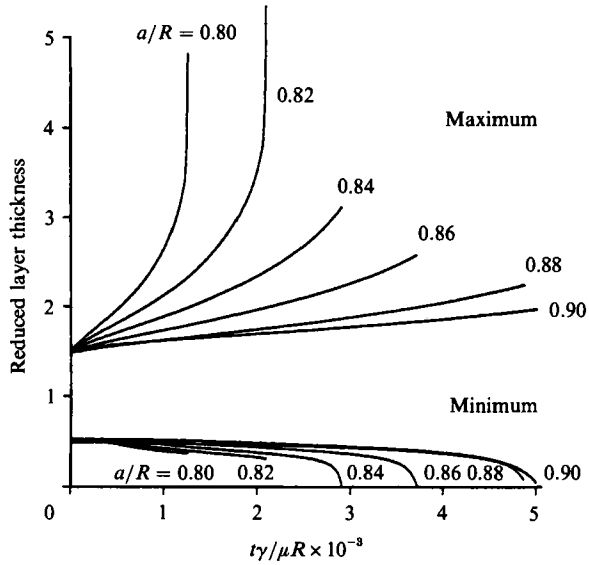

FIGURE 5. The evolution of the maximum and minimum thicknesses of thin annular layers, reduced by the initial thickness, for the most unstable disturbance.

this point we turn our attention to the behaviour of thin annular layers, with the object of determining whether the motion may lead to rupture of the layer and formation of annular lobes instead of lenses. In figure 5 we plot the maximum and minimum layer thicknesses reduced by the corresponding initial thickness, as a function of non-dimensional time $t\gamma/\mu R$ for the most unstable mode and a sequence of thin layers with $a/R = 0.80$–0.90. The initial shape of the interface is a sinusoidal wave with an amplitude of half the undisturbed layer thickness. The results indicate that for $a/R = 0.82$ the core breaks up when the annular layer has thinned to 31% of its initial thickness. For $a/R = 0.84$, however, the layer has become very thin when the radius of the core is still moderate, indicating that the layer will rupture before the core breaks up. There is similar evidence of annular-layer rupture for thinner layers. Unfortunately, the computation of the long-time evolutions for $a/R > 0.84$ had to be terminated at an intermediate stage because of the excessive time necessary to compute the Green's function at the thinnest parts of the layer.

We thus find that, for the most unstable perturbation, the annular layer will form annular lobes when $a/R > 0.82$, and lenticular bridges when $a/R < 0.82$. This threshold core radius is in good agreement with the value 0.88 suggested by Gauglitz & Radke (1988) using an approximate theory for thin layers, and in fair agreement with the value 0.91 established experimentally by the same authors and the value 0.89 suggested by Everett & Haynes (1972) using surface area minimization principles. The discrepancies are attributed to differences in initial conditions and physical properties of the fluids, as well as lack of perfect spatial periodicity.

So far we have discussed the evolution of layers subjected to perturbations corresponding to the most unstable linear mode for a given radii ratio a/R. These perturbations are expected to prevail in a natural environment. It is of interest next to examine the evolution of perturbations with values of ka different to that of the most unstable mode which are expected to prevail in a forced environment. As a test case we consider a layer with $a/R = 0.40$, subjected to perturbations with $ka = 0.500$, 0.668 (most unstable), 0.850. We find that as ka is increased, the primary

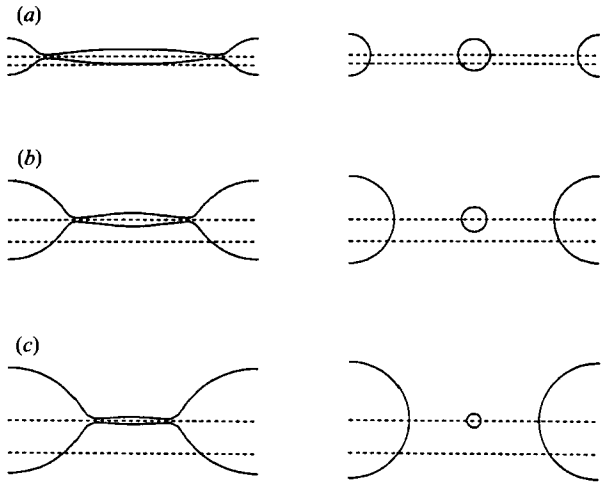

FIGURE 6. The effect of wavenumber ka on the behaviour of an unbounded thread. Advanced stages in the evolution of a thread with $\lambda = 1$ for (a) $ka = 0.218$, $t = 170$, ∞, (b) $ka = 0.5620$ (most unstable), $t = 115$, ∞, (c) $ka = 0.850$, $t = 188$, ∞.

drops obtain a more rounded shape, but the length of the connecting links remains virtually constant. For all three values of ka, almost 99% of the core fluid ends up in the primary spherical drops.

In figure 6, we illustrate a set of results for an unbounded thread, $a/R = 0$, for $ka = 0.218$, 0.562 (most unstable), 0.850 at the time when the connecting links start bulging. In the right-hand column we present the asymptotic configurations that will prevail after the links have disconnected from the primary drops and relaxed into secondary spherical droplets. We observe that as ka is increased, both the length and volume of the connecting links are reduced. In the asymptotic state shown on the right-hand column the core has transformed into an alternating array of primary and secondary drops whose volume ratio is a strong function of ka. These results indicate that the effect of ka becomes significant at low values of a/R, that is, for thick annular layers or unbounded threads.

We turn next to consider the evolution of layers subjected to a perturbation composed of two superposed waves. Our calculations show that the simultaneous growth of the two waves leads to formation of two arrays of primary drops with different volumes. We seek to establish a criterion for the distribution of the core fluid between the two primary arrays, and find it reasonable that the ratio of the radii, r_1/r_2, and ratio of volumes, v_1/v_2, of the two primary drops will depend mainly on the ratio of the linear growth rates of the two waves, α_1/α_2. To test this conjecture, in figure 7 we plot these ratios with respect to α_1/α_2 for several annular layers and unbounded threads. All data fall nearly in a straight line suggesting a universal behaviour. As the ratio of the growth rates increases, the short wave becomes progressively more important and the volume of the smaller drop is increased. When the two waves have approximately the same growth rates, the volume of the smaller drop is nearly half that of the primary drop.

3.2. *Unduloidal layers*

In the second stage of our computations we examine the behaviour of unduloidal layers whose surface is the trace of the focus of an ellipse rolling along the centreline of the tube. The shape of the unperturbed interface may be characterized by the

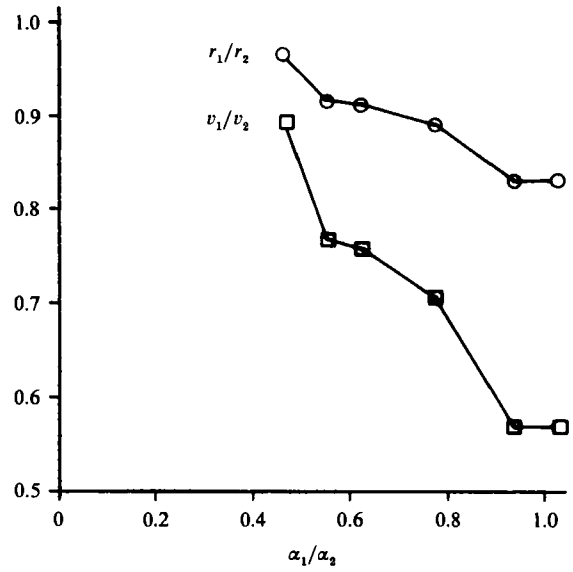

FIGURE 7. The effect of two-wave, in-phase forcing. A plot of the radii ratio, r_1/r_2, and volume ratio, v_1/v_2, of the alternating arrays of drops as a function of the ratio of the linear growth rates of the two waves, α_1/α_2.

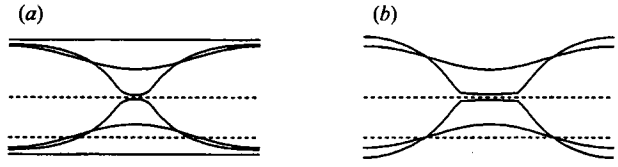

FIGURE 8. (*a*) The initial and an advanced stage in the evolution of an unduloidal layer for $a/R = 0.70$, $e = 0.2$, $ka = 1.0075$, $k\epsilon = 0.1$, and $\lambda = 1$, at $t = 0$, 311; (*b*) corresponding stages of a thread at $t = 0$, 57.

eccentricity of the ellipse, e, where $0 < e < 1$. In the limiting cases $e = 0$ and 1, the interface assumes, respectively, the shape of an infinite cylinder and the surface of an array of touching spherical drops. In our investigations, we consider perturbations whose wavelength, L, is identical to the period of the unperturbed interface.

To establish a connection between unduloidal and cylindrical layers, it is helpful to introduce the radius of the equivalent cylindrical core, $a = (V_c/\pi L)^{\frac{1}{2}}$, where V_c is the volume of the unduloidal core over one period. Non-dimensionalizing all lengths using the wavenumber $k = 2\pi/L$, we find that, apart from the viscosity ratio, the motion is a function of the radii ratio a/R, and either the eccentricity, e, or core radius ka. When $e = 0$, $ka = 1$, which corresponds to the threshold for incipient stability of a cylindrical core, and when $e = 1$, $ka = (\frac{2}{3})^{\frac{1}{2}}\pi = 2.565$, which lies within the stable regime illustrated in figure 2(*a*, *b*). In our numerical investigation, we introduce perturbations by displacing the interface in the radial direction by $\epsilon(\delta + \cos x)$, in phase with the unperturbed shape, where $k\epsilon$ ranges between 0.01 and 0.1. For a selected value of ϵ the value of δ is chosen such that the volume of the core is preserved.

In figure 8, we present the initial and an advanced shape of a layer with $a/R = 0.70$ and a thread, $a/R = 0$, for $\lambda = 1$, $e = 0.2$, or $ka = 1.0075$, and $k\epsilon = 0.1$. The lower dashed line represents the interface of the equivalent cylindrical core. This value of

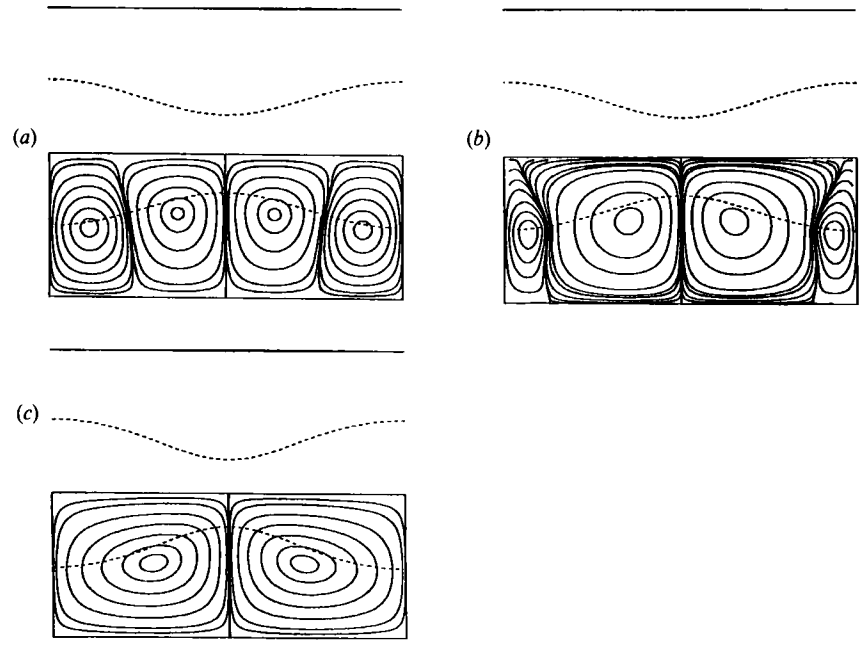

FIGURE 9. Instantaneous streamline patterns for $e = 0.2$, $a/R = 0.4$, $\lambda = 1$ at (a) $t = 0$, (b) $t = 3.75$, (c) $= 31.5$.

ka lies within the stable regime, but is very close to the threshold for neutral stability $ka = 1$. The shape of the unperturbed core is quite similar to the intermediate hourglass shape observed in the evolution of an unstable cylindrical core. In both of the cases shown in figure 8, the evolution leads to the formation of an array of primary drops connected by links. The differences between the evolutions of the layer and thread are similar to those discussed previously for cylindrical interfaces; the annular layer develops shorter links and sharper peaks.

In figure 9 we present two sequences of instantaneous streamline patterns for an unduloidal layers. In the initial stage of evolution, there are four eddies within each period, and the associated motion causes a reduction of the extrema of the interface. As the instability develops, the central eddies grow in size displacing the outer eddies to the right and left. Finally, the outer eddies disappear and the central eddies take over the motion causing the core to develop the familiar drop-link structure.

Further computations suggested that unduloidal layers are unstable, that is, there is no combination of e and a/R such that a perturbed interface returns to the original constant curvature configuration. In all cases, the cores develop drop-link structures similar to those discussed previously for the cylindrical shape. In some cases we found that the perturbation initially reduced, suggesting that the perturbation is decaying, but after a short period of decay, it began to grow. This behaviour is due to the competition between a decaying and a growing normal mode inherent in the initial perturbation.

3.3. *The effect of* λ

We turn next to investigate the effect of the viscosity ratio λ. For reasons stated earlier, we confine our attention to the unbounded thread, $a/R = 0$. In figure 10 we present advanced stages in the evolution of the most unstable mode for $\lambda = 0.1$, 1.0, and 10.0. In all three cases we observe formation of the drop-link structure. As λ is

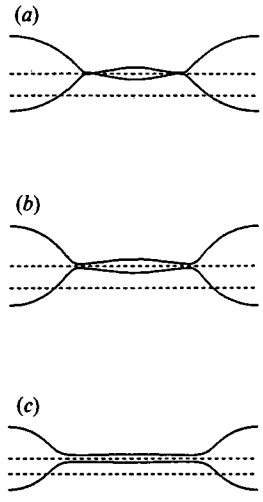

FIGURE 10. The effect of the viscosity ratio on the evolution of a thread subjected to the most unstable perturbation; (*a*) $\lambda = 0.1$, $ka = 0.5687$, $t = 37.25$, (*b*) $\lambda = 1$, $ka = 0.5620$, $t = 115$, (*c*) $\lambda = 10$, $ka = 0.4076$, $t = 418$.

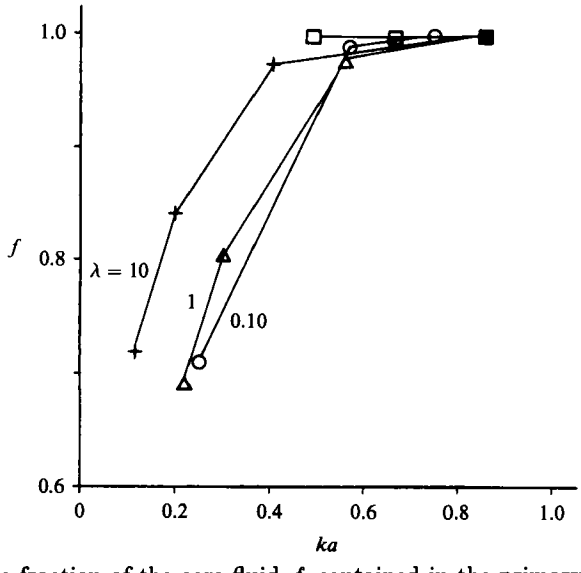

FIGURE 11. The fraction of the core fluid, f, contained in the primary drops as a function of ka for $\lambda = 0.10$, 1, 10.

increased, the link becomes longer, while the ratio of the actual rupture time to that predicted by linear stability theory increases from 1.02 at $\lambda = 0.10$, to 1.20 at $\lambda = 10$.

To examine the effect of λ on the size of the developing drops, in figure 11 we plot the fraction of the core fluid contained in the primary drops, f, as a function of ka for $\lambda = 0.10$, 1, and 10. In all cases, as ka is increased, f increases, becomes almost equal to 1 at the value of ka corresponding to the most unstable mode, and then, it remains constant. We conclude that for values of ka larger than that corresponding to the most unstable mode, λ plays a secondary role in determining the asymptotic shape of the core at large times.

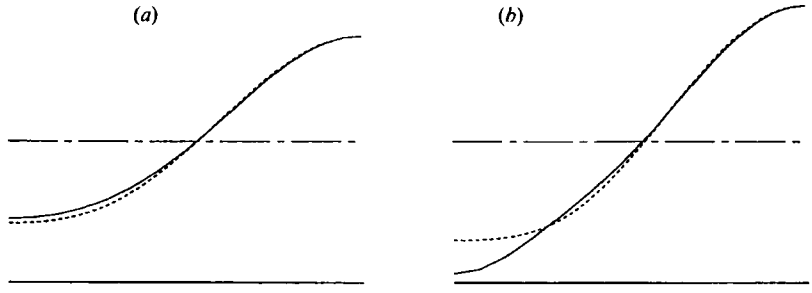

FIGURE 12. Comparison between ——, the boundary integral results and – – –, predictions of a lubrication flow model of Hammond, for $a/R = 0.90$; (a) $t = 2705$, (b) $t = 4987$. The time has been scaled with $\mu R/\gamma$.

3.4. *Comparison with approximate theories*

We have discussed the nonlinear instability of annular layers and threads and demonstrated that the motion may lead to formation of arrays of drops separated by bridges and annular lobes. Our computations provide precise information on the conditions under which these two behaviours occur, and illustrate the effect of the geometrical and physical parameters of the problem. It is of interest now to use our numerical results to assess the accuracy of previous approximate analyses.

Hammond (1983) developed an approximate theory for the evolution of a thin annular film based on the assumption of lubrication flow. His analysis proceeds by introducing the parameter $\epsilon = (R-a)/R$ and scaling the axial coordinate with the radius of the tube, R, the radial coordinate with the initial thickness of the layer, $h = R-a$, and time with $\mu R/(\gamma\epsilon^3)$. Assuming that $\epsilon \ll 1$, $\epsilon\lambda \ll 1$ and using the lubrication approximation, Hammond derived the following partial differential equation for the reduced film thickness H

$$H_t = -\tfrac{1}{3}[H^3(H_z + H_{zzz})]_z, \tag{3.1}$$

where t is the reduced time and z is the reduced axial coordinate. To leading order, the lubrication approximation disregards the flow in the core.

To compare our numerical results to the predictions of the above approximation, we solved (3.1) subject to initial and boundary conditions identical to those used in the boundary integral computations. The numerical method involves second-order finite differencing in space and an explicit method for integration in time (Newhouse 1991). Results for $a/R = 0.9$ or $\epsilon = 0.1$, when the interface is initially a sinusoidal wave with amplitude half the unperturbed film thickness are shown in figure 12. The solid and dashed curves represent, respectively, our numerical results and those produced by (3.1). Our results show that the agreement between the two computations is quite good, and that it improves as the initial thickness of the layer is decreased. The lubrication theory provides a reasonable estimate for the structure of the interface in the vicinity of the peak, but may either underestimate or overestimate the thickness of the remnant layer between the peaks. Overall, we conclude that the lubrication theory is able to capture the essential features of the motion of thin layers with $a/R > 0.90$, and may be used safely in that range. The behaviour of thin layers is discussed in detail by Hammond (1983) and Gauglitz & Radke (1988).

Next, we compare our results with those predicted by a variational theory developed by Goren (1964). The key underlying assumption in this theory is that at every instant during the evolution, the system of the two fluids will tend to minimize

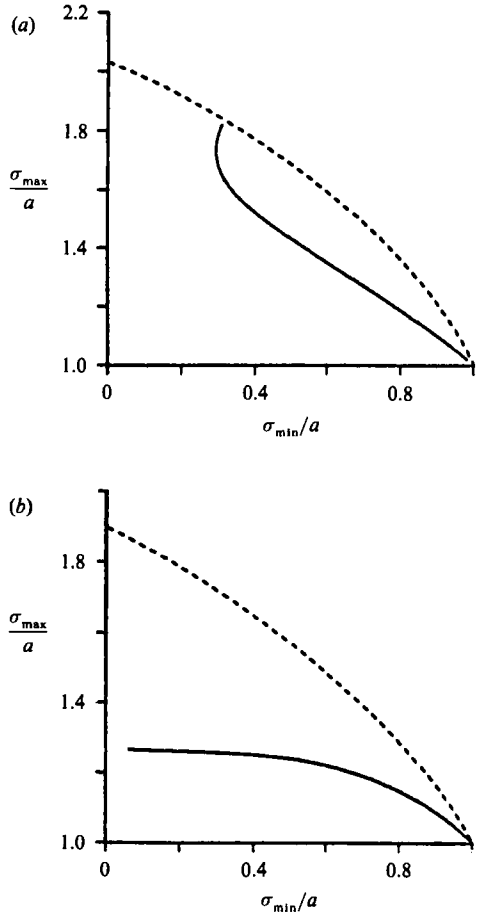

FIGURE 13. Comparison between ——, our numerical results and – – –, predictions of Goren's theory regarding the relation between the maximum and minimum core radius for (*a*) $\lambda = 1$, $a/R = 0$, (*b*) $\lambda = 1$, $a/R = 0.6$.

its free energy and thus, the area of the interface, subject to given geometrical constraints. Goren computed a family of minimum-area, periodic, axisymmetric interfaces by specifying the period and one extreme radius of the interface. These interfaces have a composite shape consisting of two drops that are connected by a perfectly cylindrical bridge; the slope and curvature of the interface are continuous at the junction. In this theory, the maximum radius of the interface is specified and the minimum radius is computed, or vice versa.

As the first test of Goren's theory, in figure 13 we plot the maximum radius versus the minimum radius (dashed line), and results from our numerical computations (solid line) for two evolutions corresponding to $\lambda = 1$ and $a/R = 0, 0.6$. In both cases, our maximum radius is less than that predicted by Goren. In the case of the unbounded thread illustrated in figure 13(*a*), the agreement between the two results improves considerably in the late stages of the motion as the core transforms into an array of drops connected by links. In the case of the annular layer illustrated in figure 13(*b*), the maximum radius increases slightly in the early stages of the evolution, but remains relatively constant as the minimum continues to decrease signalling the breakup of the core. These results suggest that the accuracy of Goren's theory will depend on the size of the core and that it may not be uniform during an evolution.

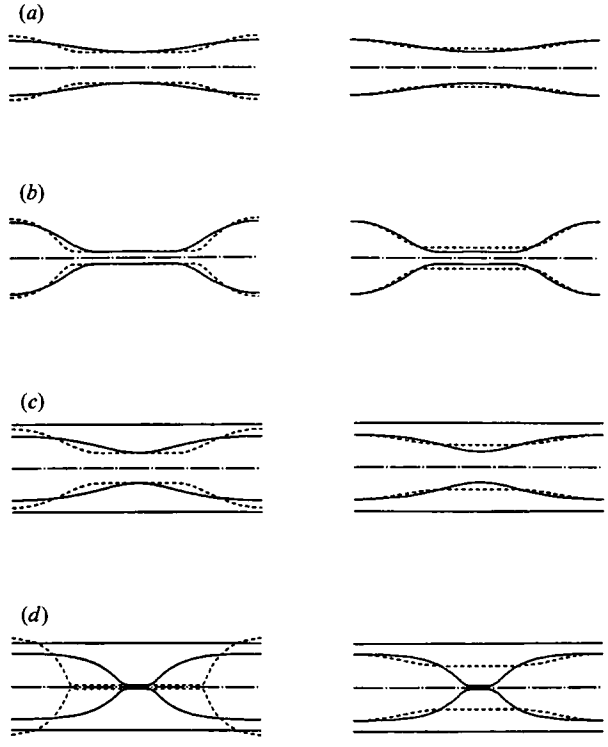

FIGURE 14. The shape of the interface ---, as predicted by Goren's theory and ——, our computations for (a) $\lambda = 1$, $a/R = 0$, $t = 77.1$, (b) $\lambda = 1$, $a/R = 0$, $t = 108.0$, (c) $\lambda = 1$, $a/R = 0.6$, $t = 901$, (d) $\lambda = 1$ $a/R = 0.6$, $t = 941$.

We present a more direct comparison between our numerical results (solid lines) and Goren's approximation (dashed lines) in figure 14, where we plot interfacial shapes at two stages in the evolution of a thread and an annular layer. In the left-hand and right-hand columns we have matched the minimum and maximum radii of the interface, respectively. In all cases, when the minimum radii are matched, the approximate interface has a longer link and a sharper contour. When the maximum radii are matched, the approximate interface has a thicker link. In general, the agreement between the numerical and approximate shapes is much better for the unbounded thread. It will be noted that in the case depicted in figure 14(*d*) the approximate interface can no longer fit inside the tube. Further computations showed that as λ increases the agreement between the numerical and approximate results improves (Newhouse 1991).

Thanks are due to the referees for their helpful comments. This work has been supported by the National Science Foundation, Grant CTS-902728, the Exxon Education Foundation, and the Eastman Kodak Company. Computer time with the San Diego Supercomputer Center was granted by the NSF and the Division of Engineering of UCSD. L. A. N. was supported partially by fellowships from the Zonta International Foundation and the Department of Education.

REFERENCES

EVERETT, D. H. & HAYNES, J. M. 1972 Model studies of capillary condensation. I. Cylindrical pore model with zero contact angle. *J. Colloid Interface Sci.* **38**, 125–137.

GAUGLITZ, P. A. & RADKE, C. J. 1988 An extended evolution equation for liquid film breakup in cylindrical capillaries. *Chem. Engng Sci.* **43**, 1457–1465.

GEORGE, R. B., LIGHT, R. W., MATTHAY, M. A. & MATTHAY, R. A. 1990 *Chest Medicine. Essentials of Pulmonary and Critical Care Medicine.* Williams & Wilkins.

GEORGIOU, E., PAPAGEORGIOU, D. T., MALDARELLI, C. & RUMSCHITZKI, D. S. 1991 The double layer–capillary stability of an annular electrolyte film surrounding a dielectric-fluid core in a tube. *J. Fluid Mech.* **226**, 149–174.

GOLDSMITH, H. L. & MASON, S. G. 1963 The flow of suspensions through tubes II. Single large bubbles. *J. Colloid Sci.* **18**, 237–261.

GOREN, S. L. 1962 The instability of an annular thread of fluid. *J. Fluid Mech.* **12**, 309–319.

GOREN, S. L. 1964 The shape of a thread of liquid undergoing break-up. *J. Colloid Sci.* **19**, 81–86.

HAMMOND, P. S. 1983 Nonlinear adjustment of a thin annular film of viscous fluid surrounding a thread of another within a circular cylindrical pipe. *J. Fluid Mech.* **137**, 363–384.

HAPPEL, J. & BRENNER, H. 1973 *Low Reynolds Number Hydrodynamics.* Martinus Nijhoff.

HU, H. & JOSEPH, D. D. 1989 Lubricated pipelining: stability of core–annular flow. Part 2. *J. Fluid Mech.* **205**, 359–396.

JOHNSON, M., KAMM, R. D., HO, L. W., SHAPIRO, A. & PEDLEY, T. J. 1991 The nonlinear growth of surface-tension driven instabilities of a thin annular film. *J. Fluid Mech.* **233**, 141–156.

KHAKHAR, D. V. & OTTINO, J. M. 1987 Breakup of liquid threads in linear flows. *Intl J. Multiphase Flow.* **13**, 71–86.

NEWHOUSE, L. A. 1991 Nonlinear instability of liquid layers. PhD thesis, University of California, San Diego.

PAPAGEORGIOU, D. T., MALDARELLI, C. & RUMSCHITZKI, D. S. 1990 Nonlinear interfacial stability of core–annular film flows. *Phys. Fluids* A **2**, 340–352.

POZRIKIDIS, C. 1990 The instability of a moving viscous drop. *J. Fluid Mech.* **210**, 1–21.

POZRIKIDIS, C. 1992*a* *Boundary Integral and Singularity Methods for Linearized Viscous Flow.* Cambridge University Press.

POZRIKIDIS, C. 1992*b* The buoyancy-driven motion of a train of viscous drops within a cylindrical tube. *J. Fluid Mech.* **237**, 627–648.

RUSSO, M. J. & STEEN, P. H. 1989 Shear stabilization of the capillary breakup of a cylindrical interface. *Phys. Fluids* A **1**, 1926–1937.

TOMOTIKA, S. 1935 On the instability of a cylindrical thread of a viscous liquid surrounded by another viscous fluid. *Proc. R. Soc. Lond.* A **150**, 322–337.